Fluorescent Bioconjugate Based on Gold Nanoparticles for the Determination of Staphylococcus aureus

Article *in* Analytical Letters · August 2016
DOI: 10.1080/00032719.2016.1212204

8 authors, including:


Leslie Susana Arcila Lozano
Instituto Politécnico Nacional
2 PUBLICATIONS **5** CITATIONS
SEE PROFILE


Rios Corripio
Colegio de Postgraduados, Cordoba, Veracruz
6 PUBLICATIONS **40** CITATIONS
SEE PROFILE


Maria Jaramillo-Flores
Instituto Politécnico Nacional
50 PUBLICATIONS **668** CITATIONS
SEE PROFILE


Rosa Rocha-Gracia
Benemérita Universidad Autónoma de Puebla
20 PUBLICATIONS **186** CITATIONS
SEE PROFILE

Analytical Letters

ISSN: 0003-2719 (Print) 1532-236X (Online) Journal homepage: http://www.tandfonline.com/loi/lanl20

Fluorescent Bioconjugate Based on Gold Nanoparticles for the Determination of Staphylococcus aureus

L. S. Arcila-Lozano, M. A. Ríos-Corripio, B. E. García-Pérez, M. E. Jaramillo-Flores, C. A. González, R. C. Rocha-Gracia, J. M. Gracia-Jiménez & M. Rojas-López

To cite this article: L. S. Arcila-Lozano, M. A. Ríos-Corripio, B. E. García-Pérez, M. E. Jaramillo-Flores, C. A. González, R. C. Rocha-Gracia, J. M. Gracia-Jiménez & M. Rojas-López (2017) Fluorescent Bioconjugate Based on Gold Nanoparticles for the Determination of Staphylococcus aureus, Analytical Letters, 50:7, 1150-1167, DOI: 10.1080/00032719.2016.1212204

To link to this article: http://dx.doi.org/10.1080/00032719.2016.1212204

Accepted author version posted online: 05 Aug 2016.
Published online: 05 Aug 2016.

ANALYTICAL LETTERS
2017, VOL. 50, NO. 7, 1150–1167
https://doi.org/10.1080/00032719.2016.1212204

Taylor & Francis
Taylor & Francis Group

FLUORESCENCE

Fluorescent Bioconjugate Based on Gold Nanoparticles for the Determination of *Staphylococcus aureus*

L. S. Arcila-Lozano[a], M. A. Ríos-Corripio[a], B. E. García-Pérez[b], M. E. Jaramillo-Flores[c], C. A. González[d], R. C. Rocha-Gracia[e], J. M. Gracia-Jiménez[f], and M. Rojas-López[a]

[a]Instituto Politécnico Nacional, CIBA-Tlaxcala, Tepetitla, Tlaxcala, México; [b]Instituto Politécnico Nacional, ENCB-Depto. de Inmunología, Ciudad de México, México; [c]Instituto Politécnico Nacional, ENCB-Depto. de Ingeniería Bioquímica, Ciudad de México, México; [d]Instituto Politécnico Nacional, ESM, Ciudad de México, México; [e]Benemérita Universidad Autónoma de Puebla, Instituto de Ciencias, Centro de Investigaciones en Ciencias Microbiológicas, Puebla, Puebla, México; [f]Benemérita Universidad Autónoma de Puebla, Instituto de Física, Puebla, Puebla, México

ABSTRACT

A practical method to determine *Staphylococcus aureus* using bioconjugated gold nanoparticles is reported. The protocol uses gold nanoparticles stabilized by tetramethylrhodamine isothiocyanate-labeled streptavidin followed by functionalization with biotinylated anti-*S. aureus* antibodies. The streptavidin-stabilized gold nanoparticles were obtained by titration and analyzed by ultraviolet–visible spectroscopy and transmission electron microscopy. The obtained fluorescent bioconjugate selectively linked to the surface of *S. aureus* in samples contaminated with the microorganism, as demonstrated by confocal micrographs. The biorecognition process was performed by mixing the fluorescent bioconjugate with the sample. Bacterial dilutions from 1 × 108 to 1 × 102 cell/ml of *S. aureus* were determined, obtaining sensitivity values of 1 × 105 cell/ml by photoluminescence and 1 × 102 cell/ml by bioimpedance. This methodology represents a useful bioanalytical approach for the determination of *S. aureus*.

ARTICLE HISTORY
Received 19 May 2016
Accepted 9 July 2016

KEYWORDS
Biosensor; gold nanoparticles; *Staphylococcus aureus*; streptavidin

Introduction

Foodborne illnesses are usually infectious or toxic in nature and caused by bacteria, viruses, parasites, or chemical substances entering the body through contaminated food or water (European Food Safety Authority, European Centre for Disease Prevention and Control 2014). The World Health Organization estimates that in 2015, 550 million (almost one in ten people in the world) fall ill and 230,000 deaths every year from diarrheal with a significant proportion of these cases following the consumption of contaminated food and drinking water. Children under 5 years of age carry 40% of the foodborne disease burden with 125,000 deaths every year (World Health Organization 2015).

Staphylococcus aureus has been indicated as the fifth causative agent of all reported outbreaks (European Food Safety Authority, European Centre for Disease Prevention and Control 2016). *S. aureus* is a ubiquitous bacterium that is both a human and zoonotic commensal and is a common cause of foodborne poisoning worldwide from the ingestion

CONTACT M. Rojas-López marlonrl@yahoo.com.mx Instituto Politécnico Nacional, CIBA-Tlaxcala, Carretera Estatal Santa Ines Tecuexcomac-Tepetitla, Km. 1.5, Tepetitla, Tlaxcala 90700, México.
Color versions of one or more of the figures in the article can be found online at www.tandfonline.com/lanl.

of heat-stable toxins produced in food (Morandi et al. 2007; Podkowik et al. 2013). The signs and symptoms of staphylococcal food poisoning occur when foods containing approximately 10^5–10^8 cells per gram or milliliter or enterotoxin (100 ng) are ingested (Sospedra et al. 2012; Wu et al. 2013). *S. aureus* may be transmitted to food by hands or drippage from the nose and mouth. Foods involved in staphylococcal food poisoning include canned mushrooms, cooked sausage, salads with eggs, meat and meat products, fowl and egg products, tuna fish, chicken, potatoes, pasta, baked goods milk, boiled goat milk, and other dairy products (González-Fandos et al. 1999; Nema et al. 2007; Normanno et al. 2007; Irlinger 2008; De Boer et al. 2009; Podkowik et al. 2013).

Conventional bacterial identification methods usually include a morphological evaluation of the microorganism as well as tests for the organisms' ability to grow in various media. Although standard microbiological techniques allow the detection of single bacteria, amplification of the signal is required through the growth of a single cell into a colony. Traditional methods for the detection of bacteria are laborious, time consuming, and material intensive (Arora et al. 2011). These involve the following steps: pre-enrichment, selective enrichment, biochemical screening, and serological confirmation. A complex series of tests is often required before the identification is confirmed. The results of such tests are often difficult to interpret and not available on the time scale desired in the microbiological laboratory. In particular way, traditional technique for identification of *S. aureus* is described in the Mexican Official Standard NOM-115-SSA1-1994 (Diario Oficial de la Federación 1995). This method allows the determination of bacteria in food and is performed directly on selective medium plates and differential culture, with confirmation by coagulase and thermonuclease protocols. The overall technique requires 4–5 days for a positive identification. This method is suitable for food analysis in which more than 100 cells of *S. aureus* bacteria are expected per gram.

Biosensors offer several advantages over existing techniques that include reduced analysis time, high throughput screening, improved sensitivity, and real-time analysis (Jasson et al. 2010). The worldwide demand for biosensors to detect microorganisms is expected to grow from $6.72 billion in 2009 to $14.42 billion by 2016 (DiGregorio 2010). The integration of nanotechnology into biosensors holds great promise for addressing the analytical needs of food diagnostic systems (Homola 2008; Sanvicens et al. 2009; Wu et al. 2013). Nanoparticles have raised great expectations in regard to generating enhanced signal-to-noise ratios, reducing response times, and use in multiplexed systems. Another advantage of nanoparticle-based technology is the detection of foodborne pathogens in unprocessed and complex food (Lin et al. 2005; Chen 2008; Lin et al. 2008; Zhu, Du, and Fu 2009; Pires et al. 2011; Wu et al. 2013; Tokel, Inci, and Demirci 2014).

Among the nanomaterials used in biosensors are gold nanoparticles, which possess unique optoelectronic properties and provide high surface-to-volume ratios with biocompatibility using appropriate ligands (Park and Hamad-Schifferli 2010; Khan et al. 2012; Sapsford et al. 2013; Soenen et al. 2015). The affinity of the surface of metallic gold nanoparticles for ligands includes thiols, disulfides, dithiocarbamates, and amines that allow bioconjugation with low-molecular-weight ligands (folic acid, thiamine, dimercaptosuccinic acid), polysaccharides (hyaluronic acid, chitosan, dextran, oligosaccharides, heparin), polyunsaturated fatty acids (palmitic acid, phospholipids), deoxyribonucleic acid oligomers, and proteins (transferrin, antibodies, lectins, cytokines, fibrinogen, thrombin) that make them scaffolds for the fabrication (Dang et al. 2005; Haiss et al. 2007;

Hun and Zhang 2007; Wampler and Ivanisevic 2009; Thanh and Green 2010; Saha et al. 2011; Sapsford et al. 2011, 2013; Chai, Tian, and Cui 2012). The affinity-based streptavidin–biotin system has been used for several applications in bionanotechnology and biosensing (Thanh and Green 2010; Chen et al. 2013; Sapsford et al. 2013). Biotin has a strong and biospecific interaction with streptavidin (dissociation constant of 10^{-15} M) and the association between biotin and streptavidin is rapid and unaffected by extremes of pH, organic solvents, and other denaturing agents (González et al. 1997; Katz 1997; Waner and Mascotti 2008).

There have been several reports on the use of gold nanoparticles to detect *S. aureus*. Some used the nonpolymerase chain reaction-based method, which measures the resonance light-scattering signal of aptamer-conjugated gold nanoparticles to detect single *S. aureus* cell within 1.5 h (Chang et al. 2013). An analytical method based on the affinity nanoprobe-based mass spectrometry that enables detection of *S. aureus* in aqueous samples was also reported. The detection limit of *S. aureus* using this method is in the order of a few tens of cells (Lai et al. 2015). A gold nanoparticle-based colorimetric aptasensor for *S. aureus* using tyramine signal amplification has been reported. The limit of the method was 9 cfu/ml (Yuan et al. 2014).

An immunochromatographic assay based on gold nanoparticles was developed for *S. aureus*. Processed food samples inoculated artificially with 0.9, 1.2, 2.4, and 6 cfu/g of bacteria yielded positive results in the immunochromatographic measurements with a total analysis time of 25 h (Huang 2007). Gold nanoparticles were used for the direct colorimetric polymerase chain reaction detection of methicillin-resistant *S. aureus* in clinical specimens. The colorimetric assay used two gold nanoparticles probes functionalized with *S. aureus* 23S rRNA- and *mecA*-specific oligonucleotides with a detection limit of 500 ng of the target amplicon (Chan et al. 2014). In a recent paper, we reported the use of gold nanoparticles covered with protein A and functionalized with fluorescent antibodies to detect salmonella (Rios-Corripio et al. 2016).

Here we describe the design of a fluorescent-nanoimmunosensor colloidal solution for the rapid identification of *S. aureus*. This system used colloidal gold nanoparticles conjugated with the labeled tetramethylrhodamine–streptavidin protein, linked to biotinylated anti-*S. aureus* antibodies. The biorecognition process used the fluorescent bioconjugate with the sample. Bacterial dilutions from 1×10^8 to 1×10^2 cell/ml of *S. aureus* were used, obtaining sensitivities of 1×10^5 cell/ml by photoluminescence and 1×10^2 cell/ml by bioimpedance measurements.

Materials and methods

Materials

Tetrachloroauric acid trihydrate 99.5% precursor was from Sigma-Aldrich. The sodium citrate dehydrate reducing agent was from J. T. Baker. The tetramethylrhodamine-conjugated streptavidin protein from *Streptomyces avidinii* was acquired from Sigma-Aldrich and was stored in pH 7.4, 0.01 M phosphate-buffered saline. Sodium chloride was purchased from Sigma-Aldrich. Anti-*S. aureus* antibody biotinylated was purchased from Abcam. The reference strain of *S. aureus* ATCC 25923 was donated from the Hospital Microbiology Laboratory and Community of Benemérita Universidad Autónoma de Puebla, México.

Bacteria preparation

Staphylococcus aureus ATCC 25923 was cultured on brain heart infusion agar plaque (Bioxon de México S. A. de C. V.) and incubated at 37°C for 12 h. A single colony was transferred into a culture tube containing 5 ml of brain heart infusion broth and incubated at 37°C for 12 h. One milliliter of the bacterial culture was centrifuged at 10,000 rpm for 10 min to obtain a pellet. The cells were washed thrice with sterile phosphate-buffered saline to remove residual medium and resuspended in 1 ml of phosphate-buffered saline. Bacterial serial dilutions were prepared for detection. The MacFarland scale was used as a standard method for the counting of bacteria. The concentration of bacteria in the initial brain heart infusion broth was estimated to be 12×10^8 cell/ml. Serial dilution was performed in sterile saline solution to 12×10^7–12×10^0 cell/ml.

Instrumentation

Ultraviolet–visible measurements were performed using an Evolution 606 Spectrophotometer (Thermo Scientific). It was used to measure the surface plasmon resonance absorption band of single nanoparticles, conjugates (gold nanoparticle–streptavidin), and bioconjugates (gold nanoparticle–streptavidin–antibody). A Philips model Tecnai 10 transmission electron microscope operated at 80 kV was used to characterize the shape and size of the gold nanoparticles and the streptavidin conjugate. A Carl Zeiss 710 confocal laser scanning microscope was used to obtain the images of *S. aureus* selectively identified by the bioconjugate.

Bioimpedance measurements used a precision impedance meter (Agilent; Model 4294A), which supplied a signal $I \cos(\omega t)$ at 100 MHz. This system was adapted by gold electrodes positioned so that the electric circuit is closed through a sample of bacteria suspended in 150 µl. Measurements were obtained from 100 Hz to 100 MHz at 181 steps spaced logarithmically.

Photoluminescence emission measurements were performed using the 375-nm excitation line of a solid-state laser Spectra-Physics, with an exit power of 16 mW, through liquid samples in a quartz cell. The emission signal from the sample was introduced into a Horiba Jobin Yvon (iHR320) monochromator with a charged coupled device detector. The 420- and 512-nm long pass filters were used to remove the laser radiation.

Synthesis of gold nanoparticles

Gold nanoparticles were prepared by chemical reduction of tetrachloroauric acid trihydrate with sodium citrate dehydrate in water. The gold nanoparticles were synthesized because the citrate ions acts as the reducing, and capping agents. This method involved the preparation of 1 ml of $HAuCl_4$ at 4% in deionized water. A quantity of 0.5 ml of this solution was added to 200 ml of deionized water and brought to boiling with constant stirring. Once the sample was between 97 and 100°C, 3 ml of 1% sodium citrate were added and the solution began to darken and turn bluish gray or purple. After 30 min, the reaction was complete and the final color of solution was a deep wine red indicating that the colloidal solution of gold nanoparticles was obtained. After the solution was cooled, the gold nanoparticles were centrifuged at 3,500 rpm for 40 min, the supernatant was removed, and the nanoparticles were resuspended in 6 ml of deionized water. The obtained suspension was stored at 4°C until use.

Titration of gold nanoparticles with streptavidin

A titration was performed to determinate the critical tetramethylrhodamine–streptavidin concentration for covering the surface of the gold nanoparticles with a full monolayer. The colloidal solution of gold nanoparticles was treated with increasing concentrations of streptavidin. After adding tetramethylrhodamine–streptavidin to the gold nanoparticles, 10% NaCl was added. If most of the gold nanoparticles were still covered with citrate groups, then the negative charge of the gold nanoparticles was screened by Na^{+} and agglomeration of the colloid took place. This flocculation was accompanied by a color change of the solution.

Preparation of the conjugate

A measure of 30 µg/ml of tetramethylrhodamine-labeled streptavidin was the minimum concentration to cover the surface of the 10–20-nm gold nanoparticles. A measure of 30 µl/ml of tetramethylrhodamine-labeled streptavidin was treated with 970 µl of gold nanoparticles, vortexed for 30 s, and incubated at room temperature for 4 min. The obtained conjugate was stored at 4°C until use.

Preparation of the fluorescent bioconjugate

A measure of 10 µg/ml of anti-*S. aureus* biotinylated antibodies was used to functionalize the surface of the fluorescent conjugate. The fluorescent conjugate was mixed with the biotinylated antibody in a 1:1 ratio and the bioconjugated nanoparticles were incubated at 37°C for 1 h. The resulting solution was centrifuged at 3500 rpm for 40 min and the supernatant was discarded. The solution was resuspended in water and stored at 4°C for the determination of *S. aureus* by fluorescence microscopy.

Preparation of bacteria

The fluorescent bioconjugate (colloidal solution) was mixed 1:1 with 1.2×10^{9} cell/ml *S. aureus*. The fluorescent bioconjugate–bacteria were incubated at 37°C for 1 h to promote the labeling of the cell membrane of *S. aureus* with the fluorescent bioconjugate. A quantity of 5 µl of the obtained suspension was placed on slides to be analyzed by fluorescence.

Results and discussion

Ultraviolet–visible absorption spectroscopy of gold nanoparticles, the conjugate, and the bioconjugate

Figure 1 shows ultraviolet–visible spectra of gold nanoparticles, the conjugate (gold nanoparticle–tetramethylrhodamine–streptavidin), and the bioconjugate (gold nanoparticle–tetramethylrhodamine–streptavidin–biotinylated antibodies). The spectrum of gold nanoparticles shows intense absorption at 520 nm, which is related with surface plasmon resonance. The spectrum of tetramethylrhodamine-labeled streptavidin protein shows three bands. The absorption at 280 nm is caused by the absorption of the aromatic amino acids tryptophan and tyrosine (Pace et al. 1995). The bands at 522 and 553 nm are

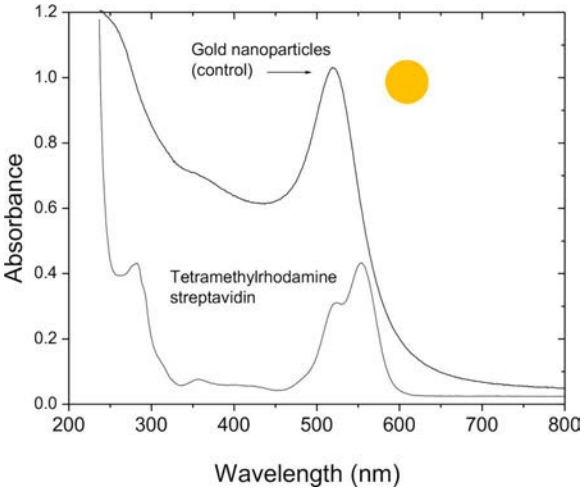

Figure 1. Ultraviolet–visible spectra of gold nanoparticles (control) and tetramethylrhodamine-labeled streptavidin protein.

associated with the absorption of the chromophore tetramethylrhodamine that labels this protein (Pedone et al. 2010; Lin et al. 2013).

For determining the concentration of protein that covers the surface of gold nanoparticles, 0–45 μg/ml of tetramethylrhodamine–streptavidin was introduced to the colloidal solution of gold nanoparticles (control) to gradually cover the surface. Once the gold nanoparticles were conjugated with the protein, the colloidal solution obtained was mixed in a 1:1 ratio with 10% NaCl to promote the aggregation of nanoparticles that were not totally covered with the protein (Geneviève et al. 2007). This procedure is known as titration. Figure 2 shows the ultraviolet–visible spectra of the gold nanoparticles conjugated with several concentrations of tetramethylrhodamine–streptavidin after mixing with NaCl. In the upper spectrum, gold nanoparticles (without streptavidin) show a broad absorption band from 700 to 800 nm due to aggregated gold nanoparticles caused by mixing with NaCl. Since the gold nanoparticles are initially covered with citrate molecules that have carboxyl groups, the negative charge of the gold nanoparticles is screened by Na^+ and colloidal aggregation occurs. This aggregation is accompanied by a change of color of the solution to gray-purple.

For concentrations between 5 and 45 μg/ml of tetramethylrhodamine–streptavidin, a superposition between the broad band associated with aggregated nanoparticles and the gold nanoparticle–streptavidin conjugate band is observed in the ultraviolet–visible spectrum. In addition, as the streptavidin concentration increases, the broad band from aggregation shifts to higher wavelength with a decrease in intensity. In the same way, as the concentration of streptavidin increases, the surface plasmon resonance absorption associated with the gold nanoparticle–streptavidin conjugate increases in intensity. However, only the spectrum of the conjugate, which is similar to the surface plasmon resonance absorption of the corresponding spectrum of the gold nanoparticle control, was displaced by 5 wavenumbers.

The spectrum of the conjugate includes the absorption of the bands at 522 and 553 nm from the chromophore tetramethylrhodamine of the streptavidin that overlap in the

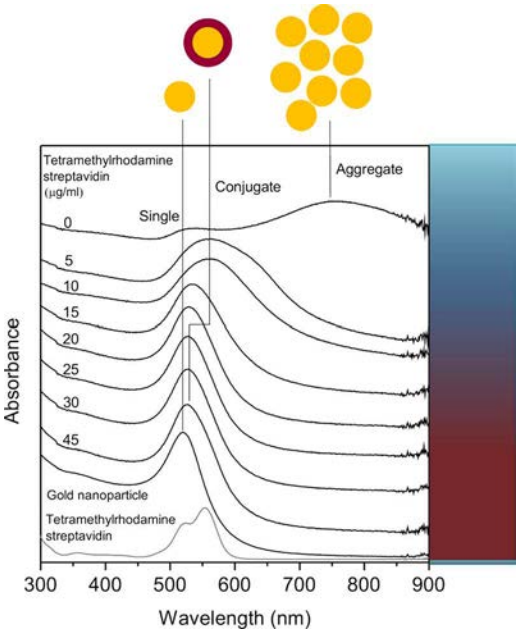

Figure 2. Ultraviolet–visible spectra of gold nanoparticles conjugated with several concentrations of tetramethylrhodamine–streptavidin during the titration.

ultraviolet–visible spectrum of each conjugate. As a consequence of the absorption of this chromophore, the linewidth of the surface plasmon resonance absorption of the conjugate (gold nanoparticle–streptavidin) was larger compared with the single gold nanoparticle control, due to damping caused by tetramethylrhodamine–streptavidin on the electronic cloud of gold nanoparticles (Sýkora et al. 2010).

The spectra with the line shape most similar to the surface plasmon resonance band of the gold nanoparticle control and without aggregation were selected to provide the optimum concentrations of tetramethylrhodamine–streptavidin to form an adequate conjugate and provide stability to the gold nanoparticles. Therefore, the concentration interval of tetramethylrhodamine–streptavidin used to cover the surface of the gold nanoparticles was from 20 to 45 μg/ml. Under these conditions, stable conjugate particles capable of withstanding the interaction with NaCl were obtained.

However, the first derivative of the ultraviolet–visible spectra of the conjugate prepared with tetramethylrhodamine–streptavidin concentrations from 0 to 45 μg/ml during the titration with NaCl highlights the main differences between the line shape of the surface plasmon resonance band of the gold nanoparticle control and the surface plasmon resonance band of the conjugate at several tetramethylrhodamine–streptavidin concentrations following reaction with NaCl. Figure 3 shows the first derivative of the ultraviolet–visible spectrum of the gold nanoparticle control and gold nanoparticles conjugated with tetramethylrhodamine–streptavidin. The signal related with the single gold nanoparticle control includes two bands. The signals of the conjugates have different line shapes and higher bandwidths. In the absence of the protein, the gold nanoparticles aggregate because their surface is uncharged following reaction with NaCl, causing a distortion of the line shape in the first derivative spectrum. When the concentration of protein increases, the surface

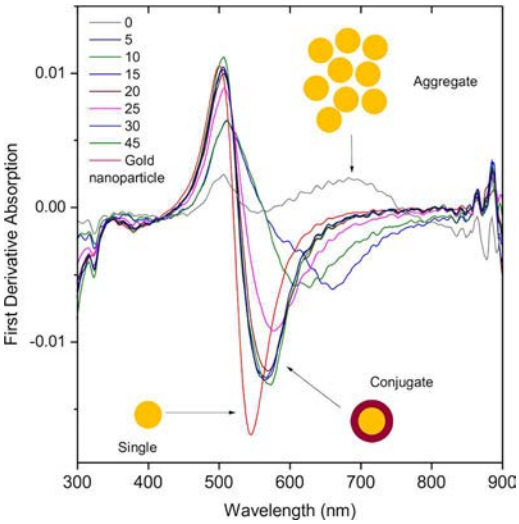

Figure 3. First-derivative absorbance of the ultraviolet–visible spectra of gold nanoparticles conjugated with tetramethylrhodamine–streptavidin (μg/ml).

of the gold nanoparticles is increasingly covered. When the concentration of protein is between 20 and 45 μg/ml, the colloidal solution does not aggregate in the presence of NaCl, and the line shapes of the first derivative spectra are similar to the controls and the red color of the colloidal solution remained.

A sufficient concentration of protein (30 μg/ml) was used to prepare the conjugate gold nanoparticle–tetramethylrhodamine–streptavidin. The conjugate structure was functionalized on the surface with biotinylated anti-*S. aureus* antibodies as described in the experimental section. The affinity between the avidin and biotin occurs so that the constant region of the biotinylated antibodies is linked to the avidin of the protein, and the variable region of the antibodies is exposed to the outside. Figure 4 shows ultraviolet–visible spectra

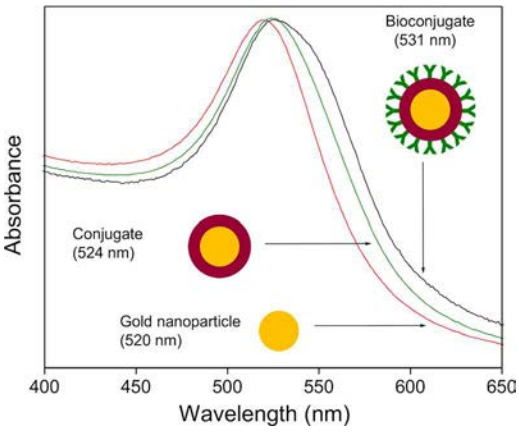

Figure 4. Ultraviolet–visible spectra of gold nanoparticles, the gold nanoparticles–tetramethylrhodamine–streptavidin conjugate, and the gold nanoparticle–tetramethylrhodamine–streptavidin–antibody bioconjugate.

of gold nanoparticle control, the gold nanoparticle–tetramethylrhodamine–streptavidin conjugate, and the gold nanoparticle–tetramethylrhodamine-streptavidin–antibody bioconjugate. The surface plasmon resonance absorption of gold nanoparticles is centered at 520 nm, while the surface plasmon resonance for the conjugate is centered at 524 nm because of frequency damping caused by tetramethylrhodamine–streptavidin. The surface plasmon resonance absorption of the bioconjugate at 531 nm also results from the shift of the wavelength to higher wavelengths by the presence of the tetramethylrhodamine–streptavidin and the biotinylated antibody linked to this protein.

Transmission electron microscopy

Gold nanoparticles and the gold nanoparticle–tetramethylrhodamine–streptavidin conjugate were characterized by transmission electron microscopy. Figure 5a shows a typical image of the gold nanoparticles used in this work. The average size was between 10 and 20 nm. Figure 5b shows a typical image of the conjugate, which is characterized by the gold nanoparticles covered by a layer of tetramethylrhodamine–streptavidin. The concentration of tetramethylrhodamine–streptavidin used to prepare this conjugate (30 μg/ml) was

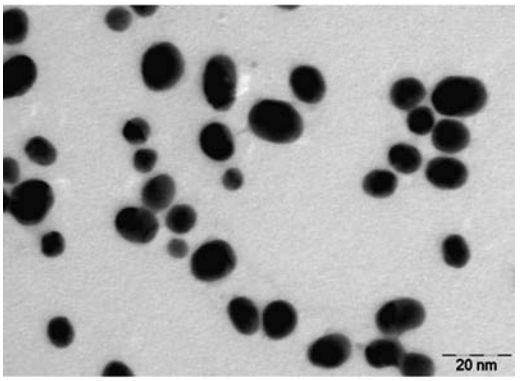

Figure 5. Transmission electron microscopy images of gold nanoparticles prepared by (a) citrate-reduction and the (b) conjugate obtained by titration with tetramethylrhodamine–streptavidin. The gold nanoparticles were covered with a layer of tetramethylrhodamine–streptavidin.

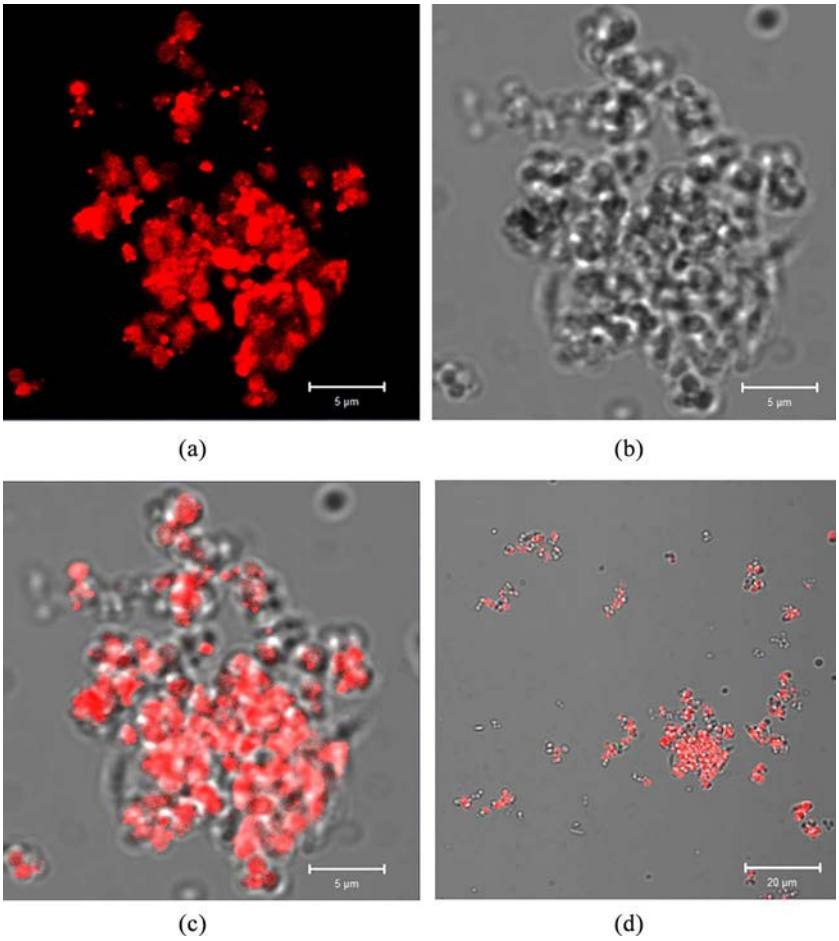

Figure 6. Confocal microscopy images of a cluster of *Staphylococcus aureus* recognized by the fluorescent bioconjugate described in this work: (a) dark-field, (b) clear-field, (c) the combination of both fields, and (d) the combination of several clusters at higher resolution.

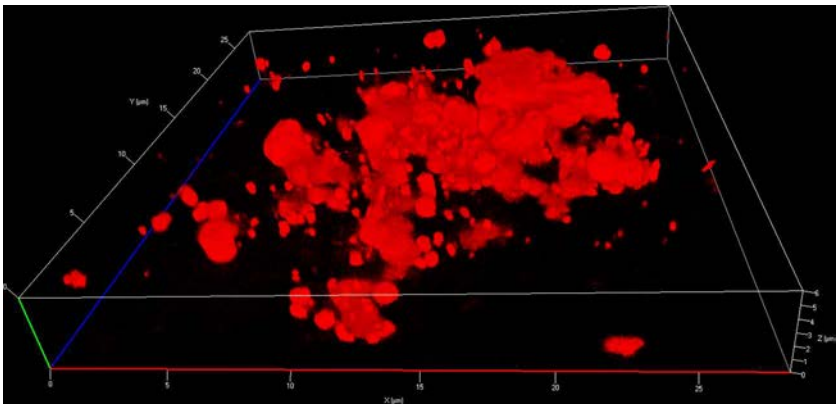

Figure 7. Three-dimensional integrated fluorescence from a cluster of S. aureus by scanning confocal microscopy. The microorganism was recognized by the fluorescent bioconjugate.

determined by the titration procedure described above. This protein layer serves to stabilize the particles in the colloidal state, promote an adequate attachment of the biotinylated antibodies during biofunctionalization, and produce the red fluorescence from the tetramethylrhodamine-chromophore.

Confocal microscopy

The fluorescent bioconjugate in colloidal form obtained in this work was directly analyzed by mixing with water treated with 10^5 cell/ml *S. aureus*. After mixing in a 1:1 ratio, an aliquot was characterized by scanning confocal microscopy. Figure 6 shows dark-field, clear-field, and the combination of both fields of a cluster of *S. aureus*. Figure 6d shows the combination of several clusters at higher magnification. In the dark field, the red

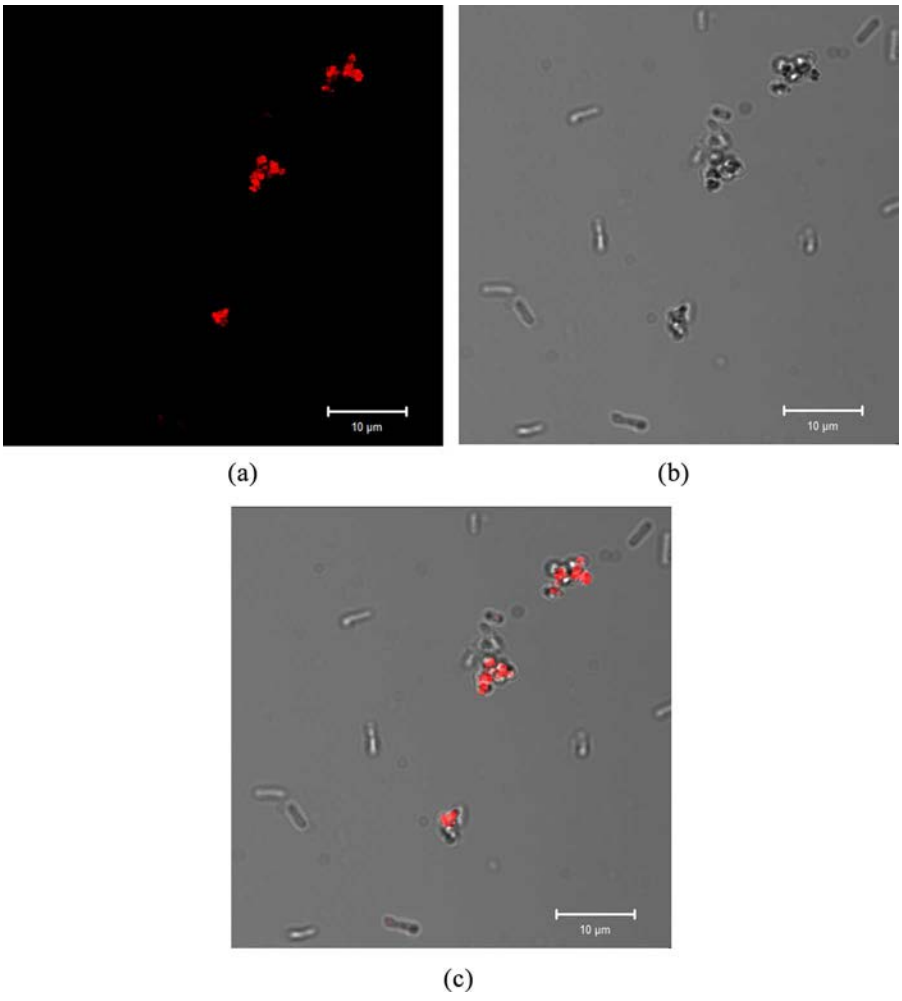

Figure 8. Confocal microscopy images of the fluorescent bioconjugate reported in this work which selectively identifies *S. aureus* in the presence of *E. coli*: (a) dark-field, (b) clear-field, and (c) combination of both fields.

fluorescence due to the tetramethylrhodamine chromophore of the streptavidin suggests adequate recognition of this pathogenic microorganism by the bioconjugate. All images were from an internal focusing plane of the cluster by integrating the fluorescence from all focusing planes. A three-dimensional reconstruction of the cluster in Figure 6a is shown in Figure 7.

Figure 8 shows images of dark, clear, and combined fields for *S.* aureus with *Escherichia coli.* Both types of bacteria are pathogenic microorganisms of interest. Fluorescence arising from the bioconjugate demonstrates selectivity for *S. aureus.* Only the surface of coccus was covered by the fluorescent biofunctionalized nanoparticle bioconjugate, unlike the *E. coli* bacilli which were not recognized by the bioconjugate. Interferences of the fluorescent bioconjugate with microorganisms depend on the cross reactivity of the antibody. The selectivity of the bioconjugate colloidal solution for *S. aureus* was favorable in the presence of pathogenic *E. coli*. However, this phenomenon needs to be further investigated to eliminate interferences with these bacteria and other *Micrococcaceae* species and to minimize nonspecific binding using different capture antibodies and blocking procedures.

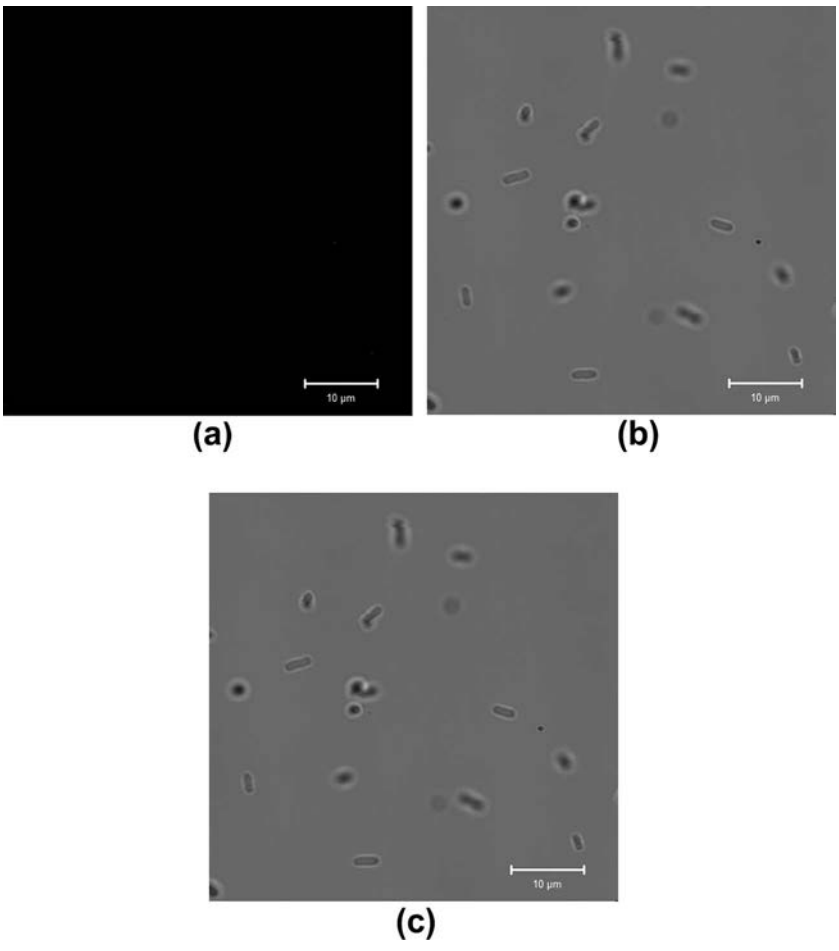

Figure 9. Confocal microscopy images of the fluorescent bioconjugate in the presence of *E. coli* with no recognition of bacilli by the bioconjugate: (a) dark-field, (b) clear-field, and (c) combination of both fields.

Figure 9 shows the negative control of this bioconjugate with *E. coli*. A quantity of 5 µl of the mixed bioconjugate–bacteria sample at 10^5 cell/ml was immobilized on slides. Micrographs of dark, clear, and combined fields show no recognition of this bacillus by the fluorescent bioconjugate. Figure 10 shows the selective biorecognition of *S. aureus* in diluted milk that was treated with *S. aureus* and *E. coli* bacteria. The bioconjugate solution was mixed 1:1 with the contaminated milk. The resultant mixture was centrifuged and immobilized on slides to be analyzed by confocal microscopy. Micrographs of dark, clear, and combined fields show the recognition of *S. aureus* by the bioconjugate. Again, only coccus was recognized by the bioconjugate and covered by the fluorescent-functionalized nanoparticles. The tetramethylrhodamine fluorescence micrographs demonstrate the presence of this pathogenic microorganism. According to these findings, this methodology may be an easy and reliable approach to determine *S. aureus* in food.

The fluorescent bioconjugate was mixed with water contaminated with *S. aureus* from 1.2×10^8 to 1.2×10^5 cell/ml and passed through cellulose acetate membranes (0.22 µm). The permeated bioconjugate nanoparticles without links to *S. aureus* were characterized

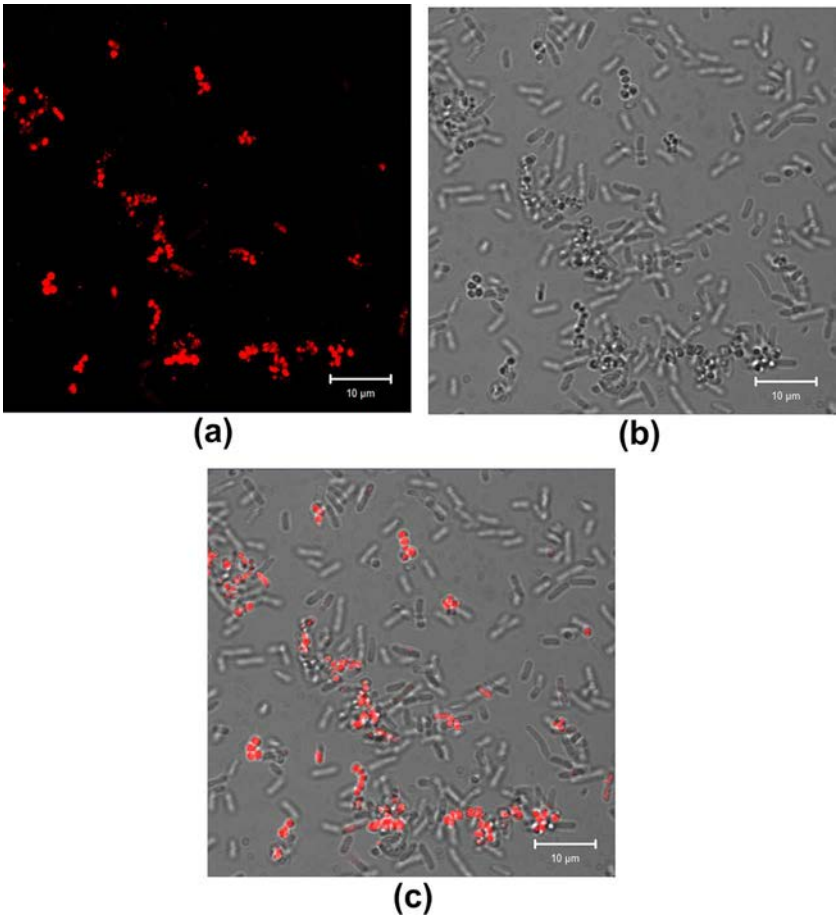

Figure 10. Confocal microscopy images of the fluorescent bioconjugate in milk contaminated with *S. aureus* and *E. coli*: (a) dark-field, (b) clear-field, and (c) combination of both fields. The selective recognition of the coccus of *S. aureus* is visible in all images.

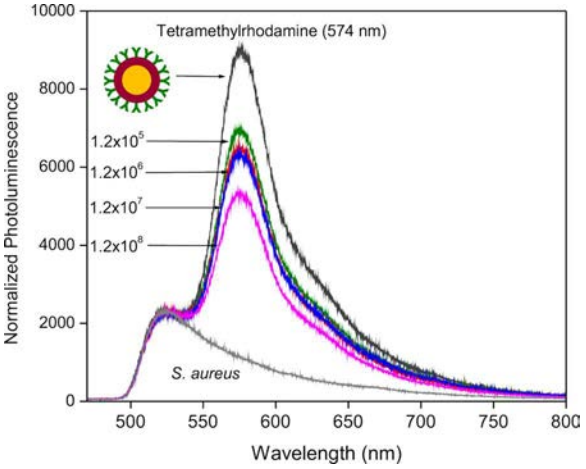

Figure 11. Photoluminescence spectra of the filtered bioconjugate nanoparticles. The retentate bioconjugate nanoparticles were linked to *S. aureus* at several concentrations of bacteria. The emission band at 574 nm is from the tetramethylrhodamine in the bioconjugate and is proportional to the bacteria concentration.

by their photoluminescence. Figure 11 shows the photoluminescence spectra of the permeated fluorescent nanoparticles that serve as emission centers during laser excitation. The filtrated samples were analyzed in a quartz cuvette, including the bioconjugate colloidal solution as the control with the bioconjugate was assigned to be 1×10^0 cell/ml by approximation. No intrinsic photoluminescence of 1.2×10^8 cell/ml *S. aureus* was observed. An intense band at 574 nm from the tetramethylrhodamine of the streptavidin in the bioconjugate nanoparticles was present. After performing spectral normalization of the band at 521 nm from the quartz cuvette, a decrease of the photoluminescence intensity

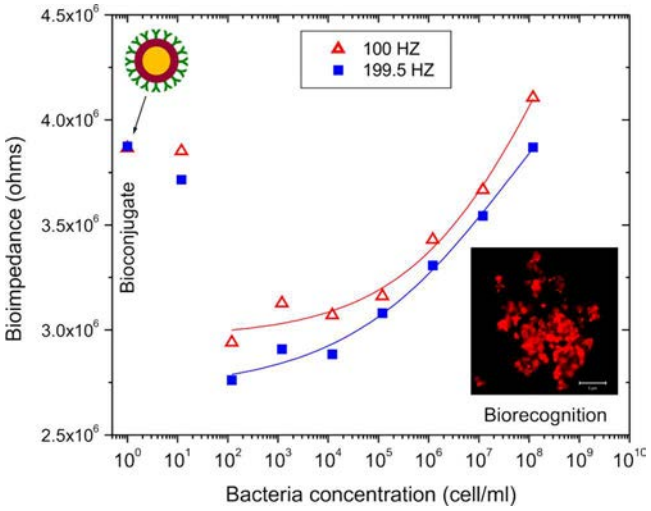

Figure 12. Bioimpedance curves of water samples contaminated with concentrations of *S. aureus* from 1.2×108–1.2×10^1 cell/ml.

was observed from the band at 574 nm with the bacteria concentration. Thus, for high-bacteria concentrations, few bioconjugated nanoparticles were obtained after filtration. On the other hand, for low-bacteria concentrations, the number of bioconjugated nanoparticles and photoluminescence increased after filtration. The sensitivity limit was 1×10^5 cell/ml.

Figure 12 shows bioimpedance curves of water treated with 1.2×10^8–1.2×10^1 cell/ml *S. aureus*. All samples were mixed in a 1:1 ratio of the bioconjugate in the colloidal solution obtained in this work. Bioimpedance measurements as a function of frequency of the electrical signal show two local maximum frequencies (not shown) at 100 and 199.5 Hz for *S. aureus* labeled with the bioconjugate. Using either frequency, a detection limit of 1×10^2 cell/ml was obtained. The signal of the bioconjugate was assigned by approximation to 1×10^0 cell/ml. An exponential dependence from a semilogarithmic plot of impedance as a function of the bacteria concentration was observed. These results show that the concentration of *S. aureus* was determined using the bioconjugate reported in this work.

Conclusion

A colloidal fluorescent bioconjugate, which is based in the use of gold nanoparticles stabilized with tetramethylrhodamine-labeled streptavidin and biofunctionalized with biotinylated anti-*S. aureus* antibody, was used for the analysis of water and milk and provided good selectivity to the surface of *S. aureus,* as evidenced by confocal microscopy. Photoluminescence emission of filtered bioconjugated nanoparticles that were previously mixed with contaminated samples provided a direct measurement of the bacteria concentration with a detection limit of 1×10^5 cell/ml. Impedance measurements of contaminated samples with this bioconjugate also provided direct determination of the bacteria concentration with a detection limit of 1×10^2 cell/ml. This methodology may be an important alternative to determine pathogens in food.

Funding

The authors thank support from SNI-CONACYT, COFAA-IPN, SIP-IPN, CNMN-IPN, and Instituto Nacional de Rehabilitación, México.

References

Arora, P., A. Sindhu, N. Dilbaghi, and A. Chaudhury. 2011. Biosensors as innovative tools for the detection of food borne pathogens. *Biosensors and Bioelectronics* 28 (1):1–12. doi:10.1016/j.bios.2011.06.002

Chai, Y., D. Tian, and H. Cui. 2012. Electrochemiluminescence biosensor for the assay of small molecule and protein based on bifunctional aptamer and chemiluminescent functionalized gold nanoparticles. *Analytica Chimica Acta* 715:86–92. doi:10.1016/j.aca.2011.12.006

Chan, W. S., B. S. Tang, M. V. Boost, C. Chow, and P. H. Leung. 2014. Detection of methicillin-resistant *Staphylococcus aureus* using a gold nanoparticle-based colourimetric polymerase chain reaction assay. *Biosensors and Bioelectronics* 53:105–11. doi:10.1016/j.bios.2013.09.027

Chang, Y. C., C. Y. Yang, R. L. Sun, Y. F. Cheng, W. C. Kao, and P. C. Yang. 2013. Rapid single cell detection of *Staphylococcus aureus* by aptamer-conjugated gold nanoparticles. *Scientific Reports* 3:1863. doi:10.1038/srep01863

Chen, Z. G. 2008. Conductometric immunosensors for the detection of staphylococcal enterotoxin B based bio-electrocalytic reaction on micro-comb electrodes. *Bioprocess and Biosystems Engineering* 31 (4):345–50. doi:10.1007/s00449-007-0168-2

Chen, Y. P., M. Q. Zou, C. Qi, M. X. Xie, D. N. Wang, Y. F. Wang, and Y. Chen. 2013. Immunosensor based on magnetic relaxation switch and biotin-streptavidin system for the detection of Kanamycin in milk. *Biosensors & Bioelectronics* 39 (1):112–7. doi:10.1016/j.bios.2012.06.056

Dang, T. X., S. J. Farah, A. Gast, C. Robertson, B. Carragher, E. Egelman, and E. M. Wilson-Kubalek. 2005. Helical crystallization on lipid nanotubes: streptavidin as a model protein. *Journal of Structural Biology* 150 (1):90–99. doi:10.1016/j.jsb.2005.02.002

De Boer, E. D., J. T. M. Zwartkruis-Nahuis, B. Wit, X. W. Huijsdens, A. J. De Neeling, T. Bosch, R. A. A. Van Oosterom, A. Vila, and A. E. Heuvelink. 2009. Prevalence of methicillin-resistant *Staphylococcus aureus* in meat. *International Journal of Food Microbiology* 134 (1–2):52–56. doi:10.1016/j.ijfoodmicro.2008.12.007

Diario Oficial de la Federación. 1995. Norma Oficial Mexicana NOM-115-SSA1–1994. Bienes y servicios. Método para la determinacioń de *Staphylococcus aureus* en alimentos. http://www.cofepris.gob.mx/MJ/Documents/Normas/115ssa1.pdf

DiGregorio, B. E. 2010. Several rapid-read microbial biosensors being developed. *Microbe* 5 (10):417–18. doi:10.1128/microbe.5.417.1

European Food Safety Authority, European Centre for Disease Prevention, and Control. 2014. The European Union summary report on antimicrobial resistance in zoonotic and indicator bacteria from humans, animals and food in 2014. *EFSA Journal* 14 (2):4380. doi:10.2903/j.efsa.2016.4380

European Food Safety Authority, European Centre for Disease Prevention, and Control. 2016. Data dictionaries—guidelines for reporting data on zoonoses, antimicrobial resistance and food-borne outbreaks using the EFSA data models for the Data Collection Framework (DCF) to be used in 2016, for 2015 data. EFSA Supporting publication 2016. http://doi:10.2903/j.efsa.2016.4380.

Geneviève, M., C. Vieu, R. Carles, A. Zwick, G. Brière, L. Salomé, and E. Trévisiol. 2007. Biofunctionalization of gold nanoparticles and their spectral properties. *Microelectronic Engineering* 84 (5–8):1710–13. doi:10.1016/j.mee.2007.01.247

González, M., L. A. Bagatolli, I. Echabe, J. L.R. Arrondo, C. E. Argaran, C. R. Cantor, and D. F. Gerardo. 1997. Interaction of Biotin with streptavidin. *Molecular Biology* 272 (17):11288–94. doi:10.1074/jbc.272.17.11288

González-Fandos, M. E., M. Sierra, M. L. García-Lopez, M. C. García-Fernández, A. Otero. 1999. The influence of manufacturing and drying conditions on the survival and toxinogenesis of *Staphylococcus aureus* in two Spanish dry sausages (chorizo and salchichón). *Meat Science* 52 (4):411–19. doi:10.1016/s0309–1740(99)00023–6. http://www.ncbi.nlm.nih.gov/pubmed/22062705.

Haiss, W., N. T. K. Thanh, J. Aveyard, and D. G. Fernig. 2007. Determination of size and concentration of gold nanoparticles from UV-vis spectra. *Analytical Chemistry* 79 (11):4215–21. doi:10.1021/ac0702084

Homola, J. 2008. Surface plasmon resonance sensors for detection of chemical and biological species. *Chemical Reviews* 108:462–93. doi:10.1021/cr068107d

Huang, S. H. 2007. Gold nanoparticle-based immunochromatographic assay for the detection of *Staphylococcus aureus*. *Sensors and Actuators B: Chemical* 127 (2):335–40. doi:10.1016/j.snb.2007.04.027

Hun, X., and Z. Zhang. 2007. A novel sensitive staphylococcal enterotoxin C1 fluoroimmunoassay based on functionalized fluorescent core-shell nanoparticle labels. *Food Chemistry* 105 (4):623–29. doi:10.1016/j.foodchem.2007.03.068

Irlinger, F. 2008. Safety Safety assessment of dairy microorganisms: Coagulase-negative staphylococci. *International Journal of Food Microbiology* 126 (3):302–10. doi:10.1016/j.ijfoodmicro.2007.08.016

Jasson, V., L. Jacxsens, P. Luning, A. Rajkovic, and M. Uyttendaele. 2010. Alternative microbial methods: An overview and selection criteria. *Food Microbiology* 27 (6):710–30. doi:10.1016/j.fm.2010.04.008

Katz, B. A. 1997. Binding of biotin to streptavidin stabilizes intersubunit salt bridges between Asp61 and His87 at low pH. *Journal of Molecular Biology* 274 (5):776–800. doi:10.1006/jmbi.1997.1444

Khan, H. A, M. A. K. Abdelhalim, M. S. Al-Ayed, and A. S. Alhomida. 2012. Effect of gold nanoparticles on glutathione and malondialdehyde levels in liver, lung and heart of rats. *Saudi Journal of Biological Sciences* 19 (4):461–64. doi:10.1016/j.sjbs.2012.06.005

Lai, H. Z., S. G. Wang, C. Y. Wu, and Y. C. Chen. 2015. Detection of *Staphylococcus aureus* by functional gold nanoparticle-based affinity surface-assisted laser desorption/ionization mass spectrometry. *Analytical Chemistry* 87 (4):2114–20. doi:10.1021/ac503097v

Lin, F. Y. H., M. Sabri, J. Alirezaie, D. Li, and P. M. Sherman. 2005. Development of a nanoparticle-labeled microfluidic immunoassay for detection of pathogenic microorganisms development of a nanoparticle-labeled microfluidic immunoassay for detection of pathogenic microorganisms. *Clinical and Vaccine Immunology* 12 (3):418–25. doi:10.1128/cdli.12.3.418–425.2005

Lin, S., H. Sharma, and M. Khine. 2013. Shrink-induced silica structures for far-field fluorescence enhancements. *Advanced Optical Materials* 1 (8):568–572. doi:10.1002/adom.201300180

Lin, Y. H., S. H. Chen, Y. C. Chuang, Y. C. Lu, T. Y. Shen, C. A. Chang, and C. S. Lin. 2008. Disposable amperometric immunosensing strips fabricated by Au nanoparticles-modified screen-printed carbon electrodes for the detection of foodborne pathogen *Escherichia coli* O157:H7. *Biosensors and Bioelectronics* 23 (12):1832–37. doi:10.1016/j.bios.2008.02.030

Morandi, S., M. Brasca, R. Lodi, P. Cremonesi, and B. Castiglioni. 2007. Detection of classical enterotoxins and identification of enterotoxin genes in *Staphylococcus aureus* from milk and dairy products. *Veterinary Microbiology* 124:66–72. doi:10.1016/j.vetmic.2007.03.014

Nema, V., R. Agrawal, D. V. Kamboj, A. K. Goel, and L. Singh. 2007. Isolation and characterization of heat resistant enterotoxigenic *Staphylococcus aureus* from a food poisoning outbreak in Indian subcontinent. *International Journal of Food Microbiology* 117:29–35. doi:10.1016/j.ijfoodmicro.2007.01.015

Normanno, G., M. Corrente, G. La Salandra, A. Dambrosio, and N. C. Quaglia. 2007. Methicillin-resistant *Staphylococcus aureus* (MRSA) in foods of animal origin product in Italy. *International Journal of Food Microbiology* 117:219–22. doi:10.1016/j.ijfoodmicro.2007.04.006

Pace, C. N., F. Vajdos, L. Fee, G. Grimsley, and T. Gray. 1995. How to measure and predict the molar absorption coefficient of a protein. *Protein Science: A Publication of the Protein Society* 4 (11):2411–23. doi:10.1002/pro.5560041120

Park, S., and K. Hamad-Schifferli. 2010. Nanoscale interfaces to biology. *Current Opinion in Chemical Biology* 14 (5):616–22. doi:10.1016/j.cbpa.2010.06.186

Pedone, A., J. Bloino, S. Monti, G. Prampolini, and V. Barone. 2010. Absorption and emission UV-Vis spectra of the TRITC fluorophore molecule in solution: a quantum mechanical study. *Physical Chemistry Chemical Physics: PCCP* 12 (4):1000–06. doi:10.1039/b920255b

Pires, A. C., N. D. F. F. Soares, L. H. M. da Silva, M. C. H. da Silva, M. V. De Almeida, M. Le Hyaric, N. J. De Andrade, R. F. Soares, A. B. Mageste, and S. G. Reis. 2011. A colorimetric biosensor for the detection of foodborne bacteria. *Sensors and Actuators: B. Chemical* 153 (1):17–23. doi:10.1016/j.snb.2010.09.069

Podkowik, M., J. Y. Park, K. S. Seo, J. Bystro, and J. Bania. 2013. Enterotoxigenic potential of coagulase-negative staphylococci. *International Journal of Food Microbiology* 163:34–40. doi:10.1016/j.ijfoodmicro.2013.02.005

Rios-Corripio, M. A., Arcila-Lozano, L. S., Garcia-Perez, B. E., Jaramillo-Flores, M. E., Hernandez-Perez, A. D., Carlos-Martinez, A. Rosales-Perez, and Rojas-Lopez, M. 2016. Fluorescent gold nanoparticle-based bioconjugate for the detection of salmonella. *Analytical Letters* 49:1862–73. doi:10.1080/00032719.2015.1128944

Saha, K., S. S. Agasti, C. Kim, X. Li, and V. M. Rotello. 2011. Gold nanoparticles in chemical and biological sensing. *Chemical Engineering Journal* 112:2739–79. doi:10.1021/cr2001178

Sanvicens, N., C. Pastells, N. Pascual, and M. P. Marco. 2009. Nanoparticle-based biosensors for detection of pathogenic bacteria. *Trends in Analytical Chemistry* 28 (11):1243–52. doi:10.1016/j.trac.2009.08.002

Sapsford, K. E., W. R. Algar, L. Berti, K. B. Gemmill, B. J. Casey, E. Oh, and I. L. Medintz. 2013. Functionalizing nanoparticles with biological molecules: Developing chemistries that facilitate nanotechnology. *Chemical Reviews* 113 (3):1904–2074. doi:10.1021/cr300143v

Sapsford, K. E., K. M. Tyner, B. J. Dair, J. R. Deschamps, and I. L. Medintz. 2011. Analyzing nanomaterial bioconjugates: A review of current and emerging purification and characterization techniques. *Analytical Chemistry* 83 (12):4453–88. doi:10.1021/ac200853a

Soenen, S. J., W. J. Parak, J. Rejman, and B. Manshian. 2015. (Intra)cellular stability of inorganic nanoparticles: Effects on cytotoxicity, particle functionality and biomedical applications. *Chemical Reviews* 115:2109–2135. doi:10.1021/cr400714j

Sospedra, I., C. Soler, J. Mañes, and J. M. Soriano. 2012. Rapid whole protein quantitation of staphylococcal enterotoxins A and B by liquid chromatography/mass spectrometry. *Journal of Chromatography* 1238:54–59. doi:10.1016/j.chroma.2012.03.022

Sýkora, D., V. Kasicka, I. Miksík, P. Rezanka, K. Záruba, P. Matejka, and V. Král. 2010. Application of gold nanoparticles in separation sciences. *Journal of Separation Science* 33 (3):372–87. doi:10.1002/jssc.200900677

Thanh, N. T. K., and L. A. W. Green. 2010. Functionalization of nanoparticles for biomedical applications. *Nano Today* 5 (3):213–30. doi:10.1016/j.nantod.2010.05.003

Tokel, O., F. Inci, and U. Demirci. 2014. Advances in plasmonic technologies for point of care applications. *Chemical Reviews* 114 (11):5728–52. doi:10.1021/cr4000623

Wampler, H. P., and A. Ivanisevic. 2009. Nanoindentation of gold nanoparticles functionalized with proteins. *Micron* 40 (4):444–48. doi:10.1016/j.micron.2009.01.002

Waner, M. J., and D. P. Mascotti. 2008. A simple spectrophotometric streptavidin-biotin binding assay utilizing biotin-4-fluorescein. *Journal of Biochemical and Biophysical Methods* 70 (6):873–77. doi:10.1016/j.jbbm.2007.06.001

World Health Organization. (2015). http://www.who.int/foodsafety/areas_work/foodborne-diseases/ferg_infographics/en/

Wu, L., B. Gao, F. Zhang, X. Sun, Y. Zhang, and Z. Li. 2013. A novel electrochemical immunosensor based on magnetosomes for detection of staphylococcal enterotoxin B in milk. *Talanta* 106: 360–66. doi:10.1016/j.talanta.2012.12.053

Yuan, J., S. Wu, N. Duan, X. Ma, Y. Xia, J. Chen, and Z. Wang. 2014. A sensitive gold nanoparticle-based colorimetric aptasensor for *Staphylococcus aureus*. *Talanta* 127:163–68. doi:10.1016/j.talanta.2014.04.013

Zhu, S., C. Du, and Y. Fu. 2009. Localized surface plasmon resonance-based hybrid Au–Ag nanoparticles for detection of *Staphylococcus aureus* enterotoxin B. *Optical Materials* 31:1608–13. doi:10.1016/j.optmat.2009.03.009